Investigation upon the performance of piezoelectric energy harvester with elastic extensions

Maoying Zhou[a,*], Yang Fu[b,c], Weiting Liu[c]

[a]*School of Mechanical Engineering, Hangzhou Dianzi University, Hangzhou, China*
[b]*School of Automation and Mechanical Systems, Zhejiang University of Science and Technology, Hangzhou, China*
[c]*State Key Lab of Fluid Power and Mechanical Systems, Zhejiang University, Hangzhou, China*

Abstract

Here in this contribution, we investigate the method of using elastic extension to tune the energy harvesting performance of classic piezoelectric cantilever energy harvesters. Dynamic model of the proposed method is established and transformed into a boundary value problem. Simulations are done to figure out the influence several system parameters, like length ratio λ_l, bending stiffness ratio λ_B, and line density ratio λ_m, upon the performance of the piezoelectric energy harvester with elastic extensions. Simulation results show that the three parameters have a combinational influence upon the performance of the proposed piezoelectric energy harvester. The addition of the elastic extension introduces extra vibration into the considered frequency range and help tune the performance of energy harvesting.

Keywords: piezoelectric energy harvesting, piezoelectric bimorph cantilever, elastic extension, performance tuning

1. Introduction

To address the urgent issues of global warming, environmental pollution, and depleting energy resources, researchers have been continuously exploring clean, renewable, and sustainable energy sources, including solar energy, bio-energy, nuclear energy and etc. [1] Extracting energy from ambient environment to power electronic devices, which is also called energy harvesting, has also been a hot research topic in the past few decades. Lots of energy harvesting devices have been put forward to convert ambiently available energy, such as vibration energy, thermal energy, solar energy, and so on, into electrical energy. [2, 3] Among all these devices, vibration energy harvesting devices have attracted the

---

*Corresponding author
    Email addresses: `myzhou@hdu.edu.cn` (Maoying Zhou), `yangfu@zju.edu.cn` (Yang Fu), `liuwt@zju.edu.cn` (Weiting Liu)

most attention due to the universal and versatile presence of vibration energy in engineering applications. [4]

According to the underlying physical principles and materials used in the devices, vibration energy harvesting devices can be classified into several categories: electromagnetic energy harvesting devices [5, 6], electrostatic energy harvesting devices [7, 8], piezoelectric energy harvesting devices [4, 9], and triboelectric energy harvesting devices [10, 11]. Owing to their simplicity of structure and ease of fabrication, piezoelectric energy harvesting devices has been the focus of many researchers in the past twenty years. [12, 3]

A classic piezoelectric energy harvester (CPEH) is composed of an elastic beam and some piezoelectric elements attached to the beam. Theoretical modelling, numerical computation, and experimental investigations have been conducted to analyze the performances of CPEHs. [13, 14] Different methods have been put forward to optimize the performance of CPEHs by changing beam shape [15], electrode coverage [16] and configuration [17], streamwise position of piezoelectric patches [18, 19], and etc. Despite all these efforts, the performance of current piezoelectric energy harvesting devices are still far from meeting the requirement of engineering applications. They are typically confronted with limited bandwidth and poor energy conversion efficiency. To improve the performance of piezoelectric energy harvesting devices, many techniques, such as resonance tuning, motion amplification, nonlinearity introduction, and so on, are presented, investigated, and analyzed. [20, 21] These researches help us obtain an indepth understanding of the piezoelectric energy harvesting mechanisms and provide useful ways to improve the performance of piezoelectric energy harvesters. However, they do not take into account the possible effect of elastic extensions, which has been shown feasible in improving output performance of piezoelectric wind energy harvesters.[22]

Here in this contribution, we focus on the influence of elastic extension upon the performance of piezoelectric energy harvesters. A piezoelectric energy harvester with attached elastic extension is put forward. Its mathematical model is derived based on Euler-Bernoulli beam model, and converted into a boundary value problem. Numerical simulations are conducted to investigate the influences of system parameters upon its performances. Results validate our proposition and provide insights into the improvement of piezoelectric energy harvesting.

2. Modeling of the proposed system

The proposed piezoelectric energy harvester with elastic extension (PEHEE) is similar to a CPEH, as shown in Figure 1. The PEHEE is made up of two parts: the primary beam and the extension beam. The primary beam is simply a CPEH, which is usually comprised of the base structure and the piezoelectric elements attached to it. Note that the primary beam is usually of a layered structure and there can be many layers of base structure as well as piezoelectric elements. Here in Figure 1, we shown the structure of a bimorph as an example. The base structure is of thickness $2h_s$ while the piezoelectric elements are of

thickness h_p. The total length of the primary beam is l_p. The extension beam is simply made from certain elastic materials, like PET. Its thickness is $2h_e$ and its length is l_e. Both the spanwise widths of the primary beam and the extension beam are set to be identical to b.
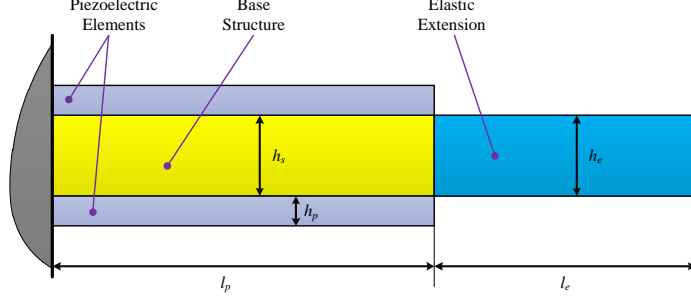

Figure 1: Schematic configuration of a piezoelectric energy harvester with elastic extension (PEHEE).

Following the classical analyzing process of piezoelectric bimorph cantilever beams [13, 14, 23], the constitutive equations for the primary beam are listed as:

$$
\begin{cases}
M_p(x_1,t) = B_p \dfrac{\partial^2 w_1(x_1,t)}{\partial x_1^2} - e_p V_p(t) \\[4mm]
q_p(x_1,t) = e_p \dfrac{\partial^2 w_1(x_1,t)}{\partial x_1^2} + \epsilon_p V_p(t),
\end{cases}
\tag{1}
$$

where $M_p(x_1,t)$ is the bending moment at the cross section of position coordinate x_1 and $q_p(x_1,t)$ is the corresponding local line charge density on the electrode. $w_1(x_1,t)$ is the displacement function of the primary beam with $0 \leq x_1 \leq l_p$ and $V_p(t)$ is the voltage across the electrodes. Considering that the piezoelectric elements are arranged in a serial connection manner [14], the coefficients B_p, e_p, and ϵ_p are defined as

$$
\begin{cases}
B_p = \dfrac{2}{3} b \left\{ E_s h_s^3 + c_{11}^E \left[(h_s + h_p)^3 - h_s^3 \right] \right\}, \\[4mm]
e_p = b e_{31} \left(h_s + \dfrac{1}{2} h_p \right), \\[4mm]
\epsilon_p = \dfrac{b \epsilon_{33}^S}{2 h_p},
\end{cases}
\tag{2}
$$

in which c_{11}^E and E_s are the elastic constants of the piezoelectric element and the base structure, respectively, e_{31} is the piezoelectric charge constant of the piezoelectric element, ϵ_{33}^S is the dielectric constant of the piezoelectric element.

Using Euler-Bernoulli assumptions [24], dynamic equations of the primary

beam are formulated as

$$B_p \frac{\partial^4 w_1(x_1,t)}{\partial x_1^4} + m_p \frac{\partial^2 w_1(x_1,t)}{\partial t^2} = 0 \tag{3}$$

where $m_p = 2b(\rho_s h_s + \rho_p h_p)$ is the line mass density of the primary beam with ρ_s and ρ_p being the volumetric density of the base structure and the piezoelectric element, respectively. Principally piezoelectric energy harvester is regarded as a current source due to its dielectric property. Hence the charge accumulation $Q_p(t)$ on the electrode is of special interest in our research. According to a simple integration process, it can be calculated as

$$Q_p(t) = \int_0^{l_p} q_p(x_1,t)\ dx_1\ =\ e_p \left[\frac{\partial w_1(x_1,t)}{\partial x_1} \right]\Big|_0^{l_p} + C_p V_p(t) \tag{4}$$

where $C_p = \epsilon_p l_p$ is the inherent capacitance of the piezoelectric layer in the primary beam. According to the Kirchhoff's law, the electric equilibrium equation is

$$\frac{dQ_p(t)}{dt} + \frac{V_p(t)}{R_l} = 0 \tag{5}$$

where R_l is the load resistance connected to the piezoelectric energy harvester.

For the extension beam, the governing equations are simply

$$B_e \frac{\partial^4 w_2(x_2,t)}{\partial x_2^4} + m_e \frac{\partial^2 w_2(x_2,t)}{\partial t^2} = 0 \tag{6}$$

where $w_2(x_2,t)$ is the displacement of the extension beam at position $0 \le x_2 \le l_e$, $B_e = \frac{2}{3}bh_e^3$ is the equivalent bending stiffness of the extension beam, $m_e = 2\rho_e h_e$ is the line mass density of the extension beam, ρ_e is the volumetric mass density of the extension beam. As a result, the defining relations for the bending moment $M_e(x_2,t)$ at the position x_2 is

$$M_e(x_2,t) = B_e \frac{\partial^2 w_2(x_2,t)}{\partial x_2^2}. \tag{7}$$

The primary beam and the extension beam are connected to each other at one end. Therefore at the joint point $x_1 = l_p$ or $x_2 = 0$, we expect the continuity of displacement functions $w_1(x_1,t)$ and $w_2(x_2,t)$, bending moments $M_p(x_1,t)$ and $M_e(x_2,t)$, and shearing forces $\frac{\partial M_p(x_1,t)}{\partial x_1}$ and $\frac{\partial M_e(x_2,t)}{\partial x_2}$. That is to say,

$$\begin{cases} w_1(l_p,t) = w_2(0,t), \\ \dfrac{\partial w_1(l_p,t)}{\partial x_1} = \dfrac{\partial w_2(0,t)}{\partial x_2}, \\ B_p \dfrac{\partial^2 w_1(l_p,t)}{\partial x_1^2} - e_p V_p(t) = B_e \dfrac{\partial^2 w_2(0,t)}{\partial x_2^2}, \\ B_p \dfrac{\partial^3 w_1(l_p,t)}{\partial x_1^3} = B_e \dfrac{\partial^3 w_2(0,t)}{\partial x_2^3}. \end{cases} \tag{8}$$

4

The left end of the primary beam is connected to the vibration sources whose vibration can be described as a function $w_b(t)$. To make it easier, we assume that the base excitation $w_b(t)$ is the only input to the system and $w_b(t)$ is strictly in the direction of $w_1(x_1, t)$ and $w_2(x_2, t)$ so that no rotation is present at the left end. As a result, we have

$$w_1(0, t) = w_b(t), \quad \frac{\partial w_1(0, t)}{\partial x_1} = 0. \tag{9}$$

At the right end of the extension beam where $x_2 = l_e$, no external forces and moments are applied and we have

$$\frac{\partial^2 w_2(l_e, t)}{\partial x_2^2} = 0, \quad \frac{\partial^3 w_2(l_e, t)}{\partial x_2^3} = 0. \tag{10}$$

With the governing equations (1,3), (2), (4), (5), (6), and (7), and the boundary conditions (8), (9), and (10), we set up a boundary value problem for the base excitation problem for the PEHEE. Generally, the problem is solved using mode decomposition method [14] or finite element method [25], where the actual motion is expressed using a series of accurate eigenmodes or approximate eigenmodes. Here in this contribution, as we are interested in the steady state response of the PEHEE, and the above described system are linear, the harmonic balance method [26] is used.

Usually we consider a base excitation $w_b(t)$ of single angular frequency σ and amplitude ξ_b, which can be expressed by $w_b(t) = Re\left\{\xi_b e^{j\sigma t}\right\}$ with $j = \sqrt{-1}$ being the imaginary unit. The amplitude ξ_b is complex and contains the phase information of the base excitation. To make things easier, we set ξ_b to be a real constant designated by the controller. Hence, according to the harmonic balance method, we can set the steady state response of the displacements $w_1(x_1, t)$ and $w_2(x_2, t)$ of the primary beam and the extension beam respectively as

$$w_1(x_1, t) = \tilde{w}_1(x_1)e^{j\sigma t}, \quad w_2(x_2, t) = \tilde{w}_2(x_2)e^{j\sigma t}, \tag{11}$$

the steady state voltage response $V_p(t)$ and charge accumulation $Q_p(t)$ as

$$V_p(t) = \tilde{V}_p e^{j\sigma t}, \quad Q_p(t) = \tilde{Q}_p e^{j\sigma t}, \tag{12}$$

and the bending moment $M_p(x_1, t)$ and $M_e(x_2, t)$ as

$$M_p(x_1, t) = \tilde{M}_p(x_1)e^{j\sigma t}, \quad M_e(x_2, t) = \tilde{M}_e(x_2)e^{j\sigma t}, \tag{13}$$

where the symbols with a hat $\sim$ denote the complex modulus of the corresponding quantities, which contains the amplitude and phase information. As a result, the above system of governing equations for the PEHEE can be summarized as

$$\begin{cases} B_p \dfrac{\partial^4 \tilde{w}_1(x_1)}{\partial x_1^4} - m_p \sigma^2 \tilde{w}_1(x_1) = 0, \\[2mm] B_e \dfrac{\partial^4 \tilde{w}_2(x_2)}{\partial x_2^4} - m_e \sigma^2 \tilde{w}_2(x_2) = 0, \\[2mm] \qquad\qquad\qquad j\sigma \tilde{Q}_p + \dfrac{\tilde{V}_p}{R_l} = 0, \end{cases} \tag{14}$$

$$\begin{cases} \tilde{M}_p(x_1) = B_p \dfrac{\partial^2 \tilde{w}_1(x_1)}{\partial x_1^2} - e_p \tilde{V}_p, \\[2ex] \tilde{Q}_p = e_p \left[\dfrac{\partial \tilde{w}_1(x_1)}{\partial x_1} \right] \Big|_0^{l_p} + C_p \tilde{V}_p, \\[2ex] \tilde{M}_e(x_2) = B_e \dfrac{\partial^2 \tilde{w}_2(x_2)}{\partial x_2^2}, \end{cases} \qquad (15)$$

and the boundary conditions become

$$\begin{cases} \tilde{w}_1(0) = \xi_b, \quad \dfrac{\partial \tilde{w}_1}{\partial x_1}(0) = 0, \\[2ex] w_1(l_p, t) = w_2(0, t), \quad \dfrac{\partial \tilde{w}_1(l_p)}{\partial x_1} = \dfrac{\partial \tilde{w}_2(0)}{\partial x_2}, \\[2ex] B_p \dfrac{\partial^2 \tilde{w}_1(l_p)}{\partial x_1^2} - e_p \tilde{V}_p = B_e \dfrac{\partial^2 \tilde{w}_2(0)}{\partial x_2^2}, \quad B_p \dfrac{\partial^3 \tilde{w}_1(l_p)}{\partial x_1^3} = B_e \dfrac{\partial^3 \tilde{w}_2(0)}{\partial x_2^3}, \\[2ex] \dfrac{\partial^2 \tilde{w}_2(l_e)}{\partial x_2^2} = 0, \quad \dfrac{\partial^3 \tilde{w}_2(l_e)}{\partial x_2^3} = 0. \end{cases} \qquad (16)$$

From the equations (14), (15), and (16), we can eliminate the electrical quantities $\tilde{Q}_p$ and $\tilde{V}_p$ by incorporating them into the boundary conditions. Actually, from equations (14) and (15), we have

$$\tilde{V}_p = \frac{j\sigma R_l e_p}{j\sigma R_l C_p + 1} \left[\frac{\partial \tilde{w}_1(x_1)}{\partial x_1} \right] \Big|_0^{l_p}, \qquad (17)$$

which can actually be used to eliminate the term $\tilde{V}_p$ in the boundary conditions (16). In the end, we can simplify the problem as a combination of the governing equations

$$\begin{cases} B_p \dfrac{\partial^4 \tilde{w}_1(x_1)}{\partial x_1^4} - m_p \sigma^2 \tilde{w}_1(x_1) = 0, \\[2ex] B_e \dfrac{\partial^4 \tilde{w}_2(x_2)}{\partial x_2^4} - m_e \sigma^2 \tilde{w}_2(x_2) = 0, \end{cases} \qquad (18)$$

and the boundary conditions

$$\begin{cases} \tilde{w}_1(0) = \xi_b, \quad \dfrac{\partial \tilde{w}_1}{\partial x_1}(0) = 0, \\[2ex] \tilde{w}_1(l_p) = \tilde{w}_2(0), \quad \dfrac{\partial \tilde{w}_1(l_p)}{\partial x_1} = \dfrac{\partial \tilde{w}_2(0)}{\partial x_2}, \\[2ex] B_p \dfrac{\partial^2 \tilde{w}_1(l_p)}{\partial x_1^2} + \dfrac{j\sigma R_l e_p^2}{j\sigma R_l C_p + 1} \dfrac{\partial \tilde{w}_1(l_p)}{\partial x_1} = B_e \dfrac{\partial^2 \tilde{w}_2(0)}{\partial x_2^2}, \quad B_p \dfrac{\partial^3 \tilde{w}_1(l_p)}{\partial x_1^3} = B_e \dfrac{\partial^3 \tilde{w}_2(0)}{\partial x_2^3}, \\[2ex] \dfrac{\partial^2 \tilde{w}_2(l_e)}{\partial x_2^2} = 0, \quad \dfrac{\partial^3 \tilde{w}_2(l_e)}{\partial x_2^3} = 0, \end{cases} \qquad (19)$$

which actually manifests as a boundary value problem.

3. Dimensionless Problem

Defining the following dimensionless variables

$$\tilde{w}_1 = \xi_b u_1, \quad \tilde{w}_2 = \xi_b u_2, \quad \tilde{x}_1 = l_p x, \quad \tilde{x}_2 = l_e x., \tag{20}$$

The above listed boundary value problem is made dimensionless. Note that here we use one independent space variable x to nondimensionalize two previously used variables x_1 and x_2. This comes from the fact that the variables x_1 and x_2 are not coupled with each other in the sense that the primary beam and the extension beam do not overlap each other except for their joint point where $x_1 = l_p$ and $x_2 = 0$. Thus the two variables do not occur in the equations simultaneously except for the boundary conditions. As for the boundary conditions, the change of variables does not affect the values of the equations. In one word, the equation (20) does not change the problem in essence. Hence, the above boundary value problem is further changed into the combination of the governing equations

$$\begin{cases} \dfrac{B_p}{l_p^4} u_1'''' - m_p \sigma^2 u_1 = 0, \\[2mm] \dfrac{B_e}{l_e^4} u_2'''' - m_e \sigma^2 u_2 = 0, \end{cases} \tag{21}$$

and the boundary conditions

$$\begin{cases} u_1(0) = 1, \quad u_1'(0) = 0, \\[2mm] u_1(1) = u_2(0), \quad \dfrac{1}{l_p} u_1'(1) = \dfrac{1}{l_e} u_2'(0), \\[2mm] \dfrac{B_p}{l_p^2} u_1''(1) + \dfrac{j\sigma R_l e_p^2}{j\sigma R_l C_p + 1} \dfrac{1}{l_p} u_1'(1) = \dfrac{B_e}{l_e^2} u_2''(0), \quad \dfrac{B_p}{l_p^3} u_1'''(1) = \dfrac{B_e}{l_e^3} u_2'''(0), \\[2mm] u_2''(1) = 0, \quad u_2'''(1) = 0, \end{cases} \tag{22}$$

in which the prime means the derivative with respect to x. The equations can again be organized in a more compact form

$$\begin{cases} u_1'''' - \nu^2 u_1 = 0, \\ u_2'''' - \nu^2 \lambda_m \lambda_l^4 / \lambda_B u_2 = 0, \end{cases} \tag{23}$$

$$\begin{cases} u_1(0) = 1, \quad u_1'(0) = 0, \\[2mm] u_1(1) = u_2(0), \quad \lambda_l u_1'(1) = u_2'(0), \\[2mm] u_1''(1) + \dfrac{j\nu\beta}{j\nu\beta + 1} \alpha^2 u_1'(1) = \lambda_B / \lambda_l^2 u_2''(0), \quad u_1'''(1) = \lambda_B / \lambda_l^3 u_2'''(0), \\[2mm] u_2''(1) = 0, \quad u_2'''(1) = 0, \end{cases} \tag{24}$$

where

$$\nu = \sigma \sqrt{\dfrac{m_p l_p^4}{B_p}}, \quad \lambda_B = \dfrac{B_e}{B_p}, \quad \lambda_m = \dfrac{m_e}{m_p}, \quad \lambda_l = \dfrac{l_e}{l_p}, \tag{25}$$

7

$$\beta = R_l C_p \sqrt{\frac{B_p}{m_p l_p^4}}, \quad \alpha = e_p \sqrt{\frac{l_p}{C_p B_p}}. \tag{26}$$

The system (23) and (24) is a two-point boundary value problem. The problem can readily be solved by a Chebyschev collocation method using the MATLAB package *Chebfun* [27].

4. Influence of extension part upon energy harvester performance

The basic geometry and material properties of the materials used in the proposed PEHEEs are summarized in Table 1. Note that some of the parameters, like length l_e, Young's modulus Y_e, and volumetric density ρ_e of the extension beam, are actually changing across different sets of simulations. The values given here are acting as a reference. In the simulation, base excitation frequency f_b and external load resistance R_l, which change the dimensionless values of ν and β, respectively, are of critical importance in the sense that these two parameters reflect the influence of vibration source and external load circuit. For every set of parameter values, we set the base excitation frequency f_b to change from $1\ Hz$ to $100\ Hz$, which covers the usual frequency range of natural vibration sources, and set the load resistance R_l to change from $1\ \Omega$ to $10\ M\Omega$, which is inspired by the Ref. [14] and takes into account the dielectric property of piezo-electric materials. Actually, when the load resistance $R_l = 1\ \Omega$, the PEHEE is said to be in a short-circuit condition as the general equivalent resistance of the PEHEE is much larger than R_l. On the other hand, when $R_l = 10\ M\Omega$, the system is close to an open-circuit condition where no external load is connected to the output electrodes.

Table 1: Geometric, material, and electromechanical parameters used in the simulation for PEHEEs

Parameter	Value
Length of the primary beam, l_p (mm)	100
Width of the PEHEE, b (mm)	20
Half thickness of the base structure, h_s (mm)	0.25
Thickness of the piezoelectric element, h_p (mm)	0.2
Young's modulus of the base structure, Y_s (Gpa)	100
Young's modulus of the piezoelectric element, Y_p (Gpa)	66
Mass density of the base structure, ρ_s (kg/m^3)	7165
Mass density of the piezoelectric element, ρ_p (kg/m^3)	7800
piezoelectric constant, d_{31} (pm/V)	-190
Permittivity, ϵ_{33}^S (nF/m)	15.93
Length of the extension beam, l_e (mm)	30
Young's modulus of the extension beam, Y_e (Gpa)	2.3
Mass density of the extension beam, ρ_e (kg/m^3)	1.38
Half thickness of the extension beam, h_e (mm)	0.25

In the following, we will investigate the influences of length l_e, Young's modulus Y_e, and volumetric density ρ_e of the beam extension upon the performance of the piezoelectric energy harvester with flexible extensions separately.

4.1. Beam extension length l_e or length ratio λ_l

The presence of the beam extension is primarily indicated by the beam extension length l_e, or equivalently the length ratio λ_l. When $\lambda_l = 0.0$, no beam extension is attached to the primary beam and the resultant piezoelectric energy harvester reduces to the classic piezoelectric energy harvesting bimorph [14], which is referred to as a reference for comparison. In this contribution, the range of length ratio λ_l to be considered is set to be $0.0 \leq \lambda_l \leq 1.0$. For each value of length ratio λ_l, the base excitation problem is solved with respect to different base excitation frequency fr and load resistance R_l. In this process, the Young's modulus of the beam extension part is set to be $Y_e = 2.3\ GPa$ while its volumetric density is set to be $\rho_e = 1.38 \times 10^3\ kg/m^3$.
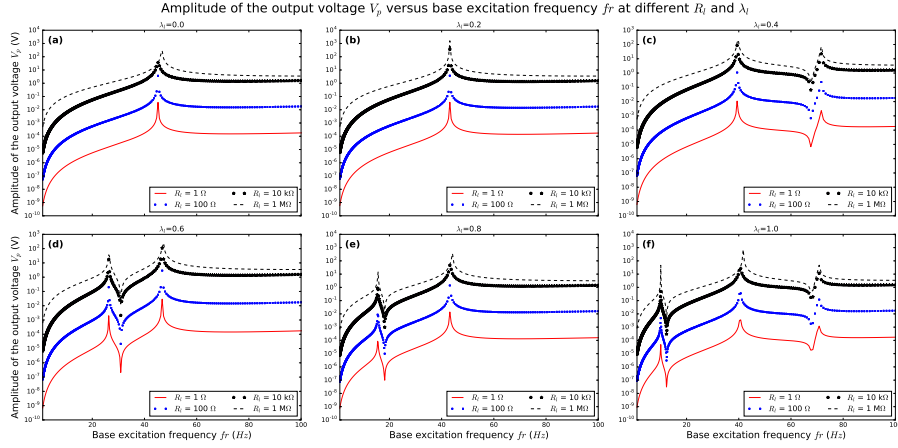
Figure 2: Output voltage V_p (amplitude) of the piezoelectric energy harvester with flexible extension versus base excitation frequency fr at different length ratio λ_l and load resistance R_l.

In the first place, we would like to explore the influence of base excitation frequency fr upon performance of the piezoelectric energy harvester at different values of load resistance R_l and length ratio λ_l. Let the frequency range of interest be $1 - 100\ Hz$. The length ratio λ_l is chosen to be 0.0, 0.2, 0.4, 0.6, 0.8, or 1.0, and load resistance R_l is chosen to be $10^0\ \Omega$, $10^2\ \Omega$, $10^4\ \Omega$, or $10^6\ \Omega$. The resulting amplitudes of output voltage V_p and output power P_p are plotted against base excitation frequency fr in Figure 2 and Figure 3, respectively. In this process, the values of beam extension part density ρ_e and Young's modulus Y_e are kept unchanged, so do the values of λ_m and λ_B.

According to Figure 2 and Figure 3, for the given values λ_B and λ_m, frequency response of the piezoelectric energy harvester in the interested frequency

Amplitude of the output power P_p versus base excitation frequency fr at different R_l and λ_l
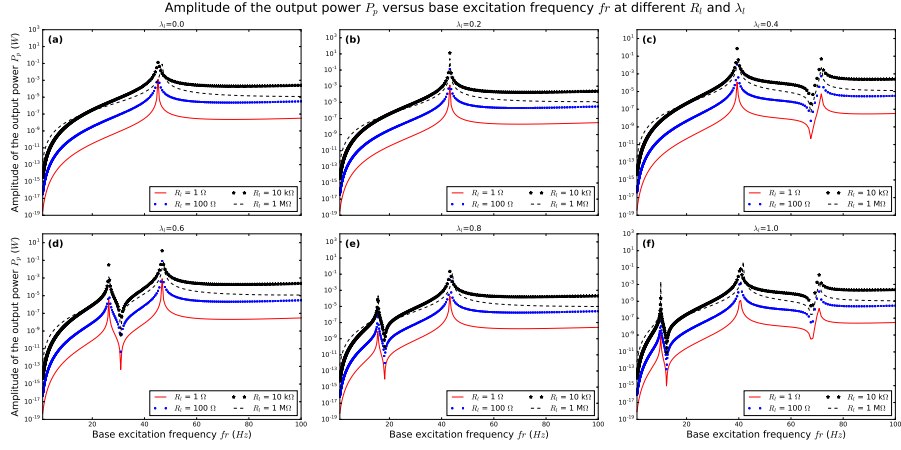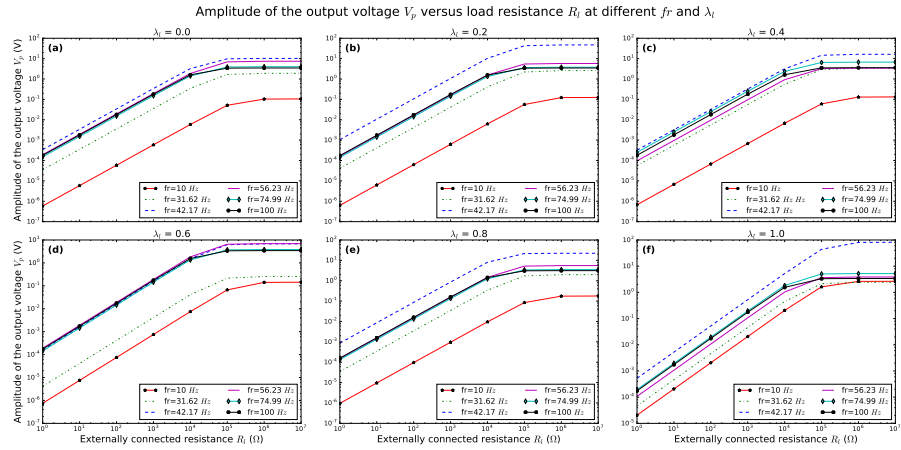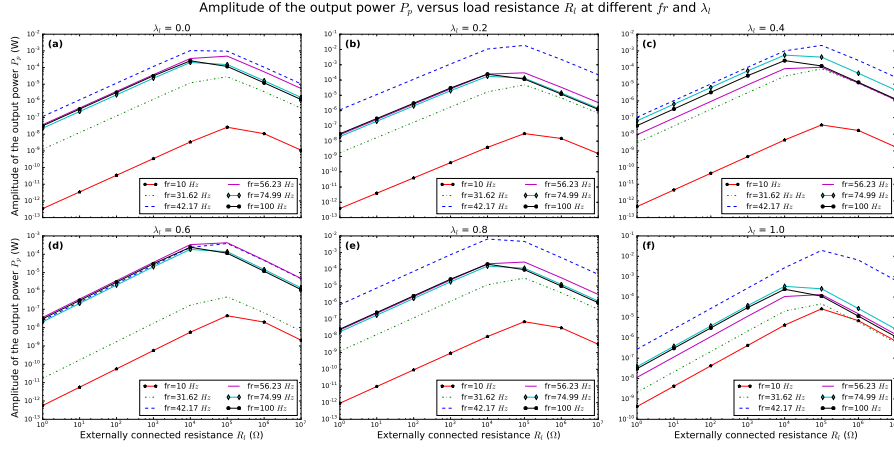

Figure 3: Output power P_p (amplitude) of the piezoelectric energy harvester with flexible extension versus base excitation frequency fr at different length ratio λ_l and load resistance R_l.

Amplitude of the output voltage V_p versus load resistance R_l at different fr and λ_l

Figure 4: Output voltage V_p (amplitude) of the piezoelectric energy harvester with flexible extension versus load resistance R_l at different frequency fr and length ratio λ_l.

Figure 5: Output power P_p (amplitude) of the piezoelectric energy harvester with flexible extension versus load resistance R_l at different frequency fr and length ratio λ_l.

range changes in accordance with the extension length l_e and thus the length ratio λ_l.

When λ_l is relatively small, say $\lambda_l = 0.2$, as shown in Figure 2(b), frequency response of the $PEHFE$ piezoelectric energy harvester with flexible extension is almost the same as that of the $CPEH$ case where $\lambda_l = 0.0$. That is to say, there is only resonant peak in the considered frequency range and the corresponding resonant frequency is around $42\ Hz$ for different values of load resistance R_l. Therefore we can conclude that in this situation, the beam extension part is playing a negligible role in the motion of the primary beam part. As a result, energy harvesting performances of the proposed piezoelectric energy harvesters with flexible extensions are similar to that of a classic piezoelectric energy harvester.

With the increase of the length ratio λ_l, say $\lambda_l = 0.4$, 0.6, or 0.8, as shown in Figure 2(b), (c), and (d), respectively, there begins to exist an extra resonant and anti-resonant mode in the considered frequency range, compared with that of the case of no flexible extension where $\lambda_l = 0.0$. An increase of the value of λ_l causes the decrease of the resonant and anti-resonant frequencies of the newly occurring mode. What's more, for the cases of $\lambda_l = 0.4$ and 0.6, the resonant frequency of the previously existing mode, which corresponds to the first resonant mode of a classic piezoelectric energy harvester, is shifted by an obvious degree. This can be explained as follows. The motion of the proposed piezoelectric energy harvester with flexible extension is controlled by the primary beam part and the beam extension part. With the increase of λ_l, resonant frequency of the beam extension part approaches that of the primary beam. Thus the two parts interact with each other at a high level. resonant frequency of the whole piezoelectric energy harvester with flexible extension is therefore tuned by the beam extension part. When the resonant frequency of the beam
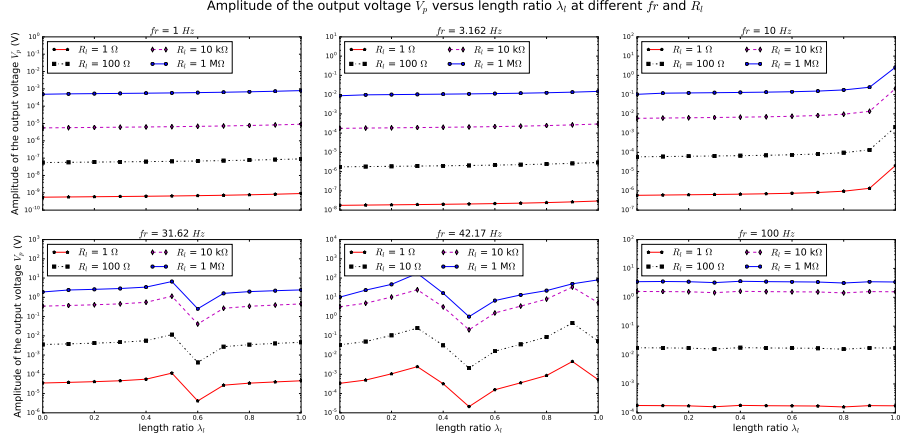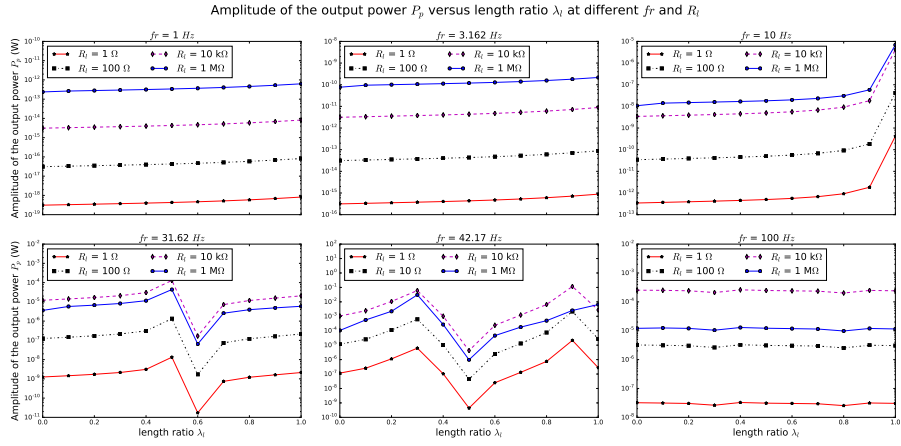
11

Figure 6: Output voltage V_p (amplitude) and output power P_p (amplitude) of the piezoelectric energy harvester with flexible extension versus length ratio λ_l at different frequency f and load resistance R_l. to be revised in the legend, add label (a), (b)

Figure 7: Output voltage V_p (amplitude) and output power P_p (amplitude) of the piezoelectric energy harvester with flexible extension versus length ratio λ_l at different frequency f and load resistance R_l. to be revised in the legend, add label (a), (b)

12

extension is far small than that of the primary beam, which is the case for $\lambda = 0.8$, as shown in Figure 2(d), the two parts have little effect upon each other.

If we further increase the length ratio to $\lambda_l = 1.0$, more resonant and anti-resonant modes occur in the considered frequency range. It can be found from Figure 2(d) and Figure 3(d) that, amplitude of the output voltage V_p and output power P_p at the newly occurring resonant mode is comparable in order of magnitude to that of the classic piezoelectric energy harvester.

In this view, attachment of the flexible extension part actually increases the working frequency range of the piezoelectric energy harvester, as typical piezoelectric energy harvesters rely on resonant modes to work. On the other hand, the flexible extension also provides a way to tune the bandwidth of a piezoelectric energy harvester. An obvious way to do so is to choose the parameters of the beam extension part, so that the beam extension part and the primary beam part have similar resonant frequency and interact strongly with each other. The point to be noticed is the existence of anti-resonant modes. They correspond to low output voltage and output power, and to some degree narrows the bandwidth of the energy harvester. However, it is still not worse than an otherwise non-resonant vibration, as in both cases the electrical output of the piezoelectric energy harvester is unusable.

In the second place, we investigate the influence of load resistance R_l upon performance of the piezoelectric energy harvester at different values of base excitation frequency fr and length ratio λ_l. The resulting amplitudes of output voltage V_p and output power P_p are shown in Figure 4 and Figure 5, respectively. It is obvious that in the range of low R_l, a power law exists between the amplitudes of output voltage V_p and output power P_p and load resistance R_l. For all the chosen values of base excitation frequency fr, the increase of R_l leads to an increase in V_p. Ultimately, V_p approaches asymptotically to a limit value V_p^{lim}. This value actually corresponds to the amplitude of open-circuit output voltage of the piezoelectric energy harvester. At the same time, the value of P_p exhibits an obvious maximum at some values of R_l between 10 $k\Omega$ and 1 $M\Omega$. And on both sides away from the maximum value, we see also a power law between the value of R_l and P_p, as shown in Figure 5. This indicates that an asymptotic analysis may help us to simplify the analysis of performance of piezoelectric energy harvesters. But this is out of the scope of our current contribution and will be covered in the future research.

In the third place, at different values of fr and R_l, we directly plot the amplitudes of V_p and P_p with respect to λ_l, which are shown in Figure 6 and Figure 6, respectively. It is shown that at given values of R_l and fr, output performances of the proposed piezoelectric energy harvesters can be tuned by the parameter λ_l. For example, when $fr = 31.62 \ Hz$ and $R_l = 10 \ k\Omega$, a maximum peak of V_p and P_p is found around $\lambda_l = 0.5$. Compared with the case of no flexible extension ($\lambda_l = 0$), the amplitude of output voltage V_p is about 13 times larger, while the amplitude of output power P_p is about 3 times larger. Similar phenomena can be found when $fr = 42.17 \ Hz$. This indicates that the addition of the flexible extension can substantially increase the output

13

performance of a piezoelectric energy harvester. It should be noted that in case of large values of fr, like $fr = 100\ Hz$, the tuning performance of the flexible extension is no longer significant.

4.2. Beam extension Young's modulus Y_e or bending stiffness ratio λ_B

To investigate the influence of bending stiffness ratio λ_B upon the performance of the piezoelectric energy harvester with flexible extension, we set different values of Young's modulus Y_e of the beam extension part to change the values of λ_B. Considering the properties of commonly used engineering materials [28], the values of Y_e is set to be in the range of $0.01\ GPa \leq Y_e \leq 400\ GPa$. For each value of bending stiffness ratio λ_B, the base excitation problem is solved with respect to different base excitation frequency fr and load resistance R_l. In this process, the length ratio is fixed to be $\lambda_l = 0.3$ while its volumetric density is set to be $\rho_e = 1.38 \times 10^3\ kg/m^3$.

Firstly, the influence of base excitation frequency fr upon performance of the piezoelectric energy harvester is shown Figure 8 and Figure 9 at different values of load resistance R_l and bending stiffness ratio λ_B. To have a clear clue about the value of λ_B, it is found that for a Young's modulus of $Y_e = 0.01\ GPa$, the corresponding value of bending stiffness ratio is $\lambda_B = 2.39 \times 10^{-5}$, while for a Young's modulus of $Y_e = 200\ GPa$, the corresponding value of bending stiffness ratio is $\lambda_B = 0.478$.
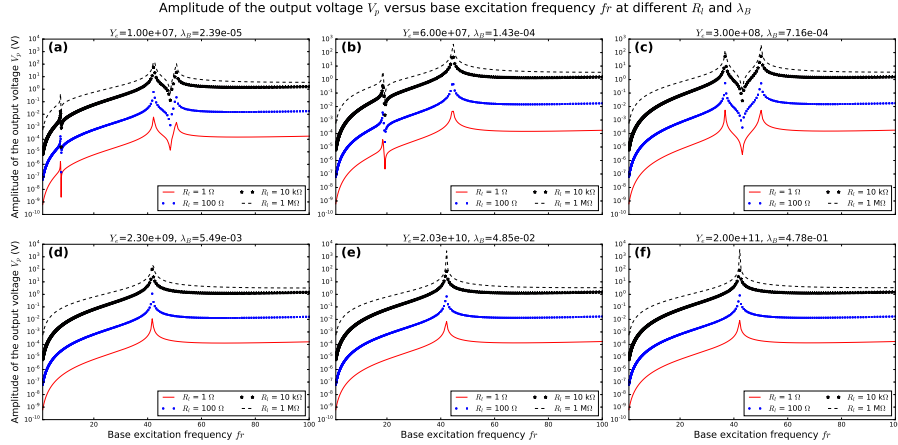

Figure 8: Output voltage V_p (amplitude) of the piezoelectric energy harvester with flexible extension versus base excitation frequency fr at different bending stiffness ratio λ_B and load resistance R_l. to be revised in the legend. change figure title

It is easily seen from Figure 8 and Figure 9 that, at the given values of λ_l and λ_m, bending stiffness ratio λ_B also affects frequency response of the proposed piezoelectric energy harvester with flexible extension, but in a different manner from length ratio λ_l.
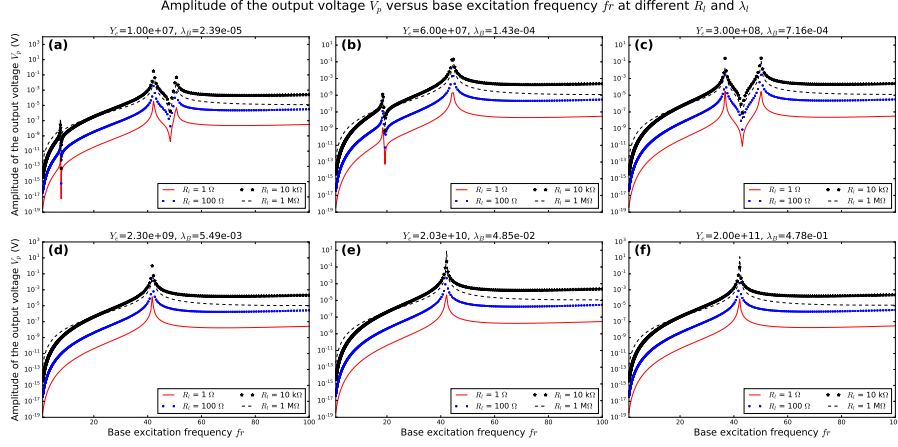
14

Figure 9: Output power P_p (amplitude) of the piezoelectric energy harvester with flexible extension versus base excitation frequency fr at different bending stiffness ratio λ_B and load resistance R_l. to be revised in the legend. change figure title

When the bending stiffness ratio λ_B is very small, say $Y_e = 0.01\ GPa$, as shown in Figure 8(a) and Figure 9(a), there exist multiple resonant modes in the considered frequency range. And some of the resonant modes are potential to be used for energy harvesting. With the increase of bending stiffness ratio λ_B, fewer resonant modes are present in the considered frequency range. For example, when $Y_e = 0.3\ GPa$, two resonant modes are present and when $Y_e = 2.3\ GPa$, only one resonant mode is present. As a result, less frequencies can be utilized for energy harvesting. That is to say, to achieve an energy harvesting capacity of wider frequency range, smaller bending stiffness ratio λ_B is preferred. Actually, from Figure 8 we can conclude that, a bending stiffness ratio λ_B in the order of 10^{-4} or lower is beneficial to the energy harvesting performance of the piezoelectric energy harvester with flexible extension. However, only changing the value of λ_B is not the best way to tune the energy harvesting performance of the piezoelectric energy harvester with flexible extension. It is seen from the previous subsection and this subsection that, the combination change of larger λ_l and lower λ_B serve better for this goal.

Similarly, for a set of chosen values of Y_e and therefore λ_B, we plot the amplitudes of output voltage V_p and output power P_p with respect to load resistance R_l at different base excitation frequencies fr in Figure 10 and Figure 11, respectively. It is easily seen that the amplitude of output voltage V_p increases in terms of increasing R_l and ultimately reaches a limit, which is actually the open-circuit output voltage. The amplitude of output power P_p will reaches its maximum at a critical value of R_l, which is dependent on the values of λ_B and fr.

The influence of bending stiffness ratio λ_B is shown by plotting the amplitudes of output voltage V_p and output power P_p relative to λ_B at different values

15
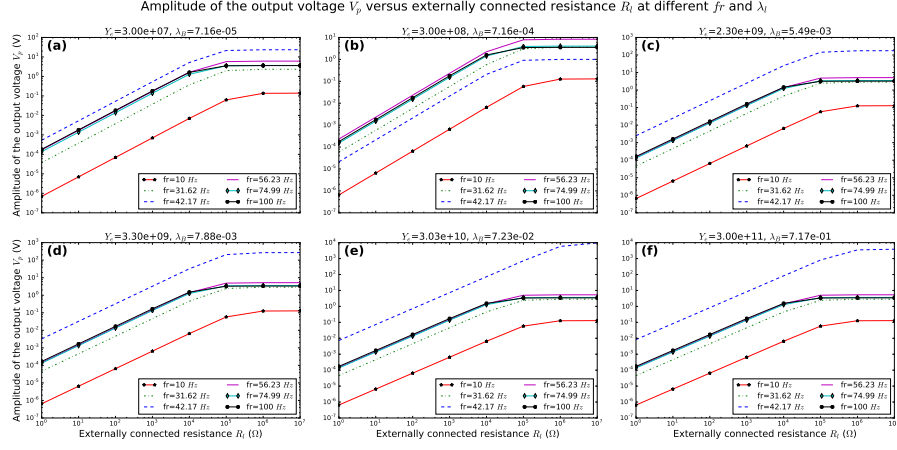
Figure 10: Output voltage V_p (amplitude) of the piezoelectric energy harvester with flexible extension versus bending stiffness ratio λ_B at different frequency fr and load resistance R_l. to be revised in the legend. change figure title
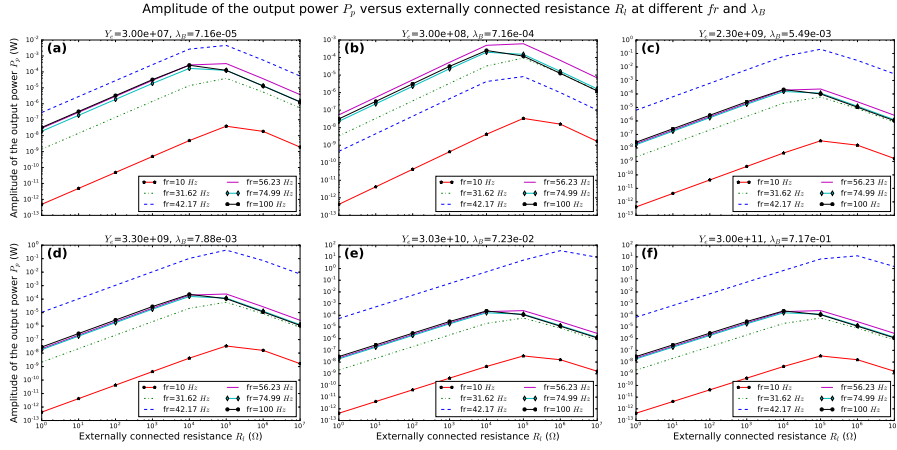

Figure 11: Output power P_p (amplitude) of the piezoelectric energy harvester with flexible extension versus bending stiffness ratio λ_B at different frequency fr and load resistance R_l. to be revised in the legend. change figure title

16

of load resistance R_l and base excitation frequency fr, as shown in Figure 12 and Figure 13, respectively. It is found that for a low frequency base excitation, as shown in Figure 12(a) and (b), no big difference is seen when we change the values of λ_B. The amplitudes of output voltage V_p and output power P_p remain at a low level and the proposed piezoelectric energy harvester with flexible extension can not be used for energy harvesting. For a higher base excitation frequency fr, as shown in Figure 12(c) and (d) and Figure 13(c) and (d), a peak of V_p and P_p is found for certain value of λ_B. The output performance of the piezoelectric energy harvester with flexible extension is increased by changing the value of λ_B. For a further higher value of fr, as shown in Figure 12(e), the value of λ_B significantly change the amplitudes of output voltage V_p and output power P_p. To achieve higher energy harvesting performance, higher (in the order of 10^{-1}) or lower (in the order of 10^{-5}) values of λ_B are preferred against a moderate (in the order of 10^{-3}) value of λ_B. For the value of base excitation frequency $fr = 100\ Hz$, as shown in Figure 12(f), the value of λ_B is found again playing a minor role in changing the values of V_p and P_p.
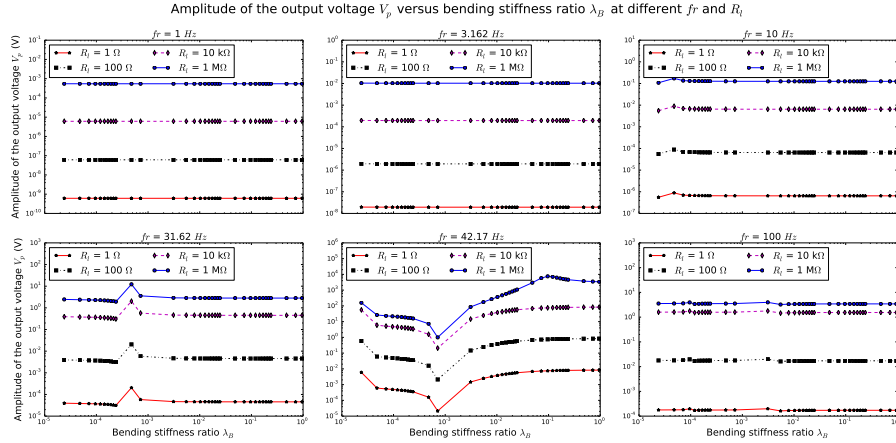

Figure 12: Output voltage V_p (amplitude) of the piezoelectric energy harvester with flexible extension versus bending stiffness ratio λ_B at different frequency fr and load resistance R_l.

4.3. Beam extension line density ρ_e or line density ratio λ_m

To investigate the influence of line density ratio λ_m upon the performance of the piezoelectric energy harvester with flexible extension, the volumetric density ρ_e of the beam extension part is changed according the properties of commonly used engineering materials [28]. For the convenience of performance comparison, ρ_e is set to be $1.38 \times 10^1\ kg/m^3$, $1.38 \times 10^2\ kg/m^3$, $1.38 \times 10^4\ kg/m^3$, or $1.38 \times 10^5\ kg/m^3$. For each value of line density ratio λ_m, the base excitation problem is solved for different base excitation frequency fr and load resistance R_l. During the simulation, the length ratio is fixed to be $\lambda_l = 0.3$ while the beam extension bending stiffness is set to be $Y_e = 2.3\ GPa$.
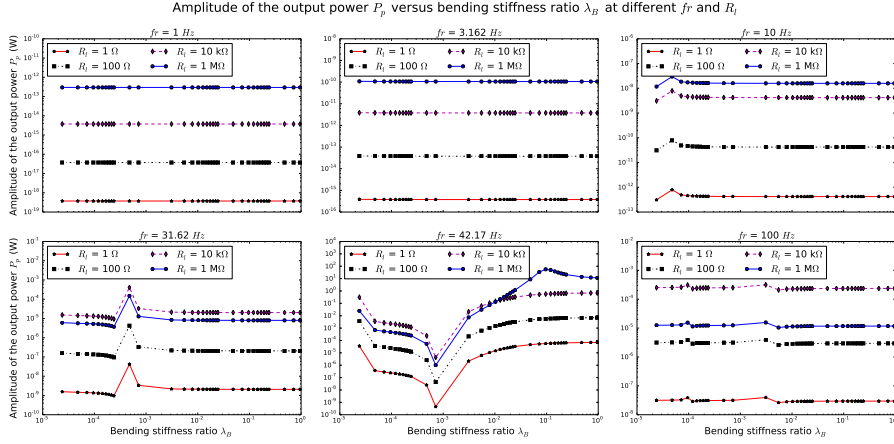
17

Figure 13: Output power P_p (amplitude) of the piezoelectric energy harvester with flexible extension versus bending stiffness ratio λ_B at different frequency fr and load resistance R_l.

The influence of base excitation frequency fr upon performance of the piezoelectric energy harvester is shown Figure 14 and Figure 15 at different values of load resistance R_l and bending stiffness ratio λ_B. A simple calculation shows that when $\rho_e = 1.38 \times 10^1\ kg/m^3$, $\lambda_e = 1.03 \times 10^{-3}$, while for $\rho_e = 1.38 \times 10^4\ kg/m^3$, $\lambda_m = 1.03$. For typical flexible like PET[29], ρ_e is $1.38 \times 10^1\ kg/m^3$, calculation results shown in Figure 14(c) and Figure 15(c) indicate that no extra resonant modes are present in the considered frequency range. Besides, no big difference is observed in terms of the amplitudes of output voltage V_p and output power P_p compared with the cases with lower volumetric densities, as shown in Figure 14(a) and (b) and Figure 15(a) and (b). However, for a larger density ρ_e, as shown in Figure 14(d) and Figure 15(d), the existence of extra resonant modes is seen. As a result, we can conclude that a heavier beam extension may be better for energy harvesting, but it is not always possible to find appropriate materials. Indeed, for most structure materials in engineering applications, the corresponding volumetric densities are not enough to generate extra resonant modes in the range. Hence, it is not wise to depend on the parameter ρ_e only to effectively tune the performance of the energy harvester with flexible extension.

A second plot is done between the amplitudes of output voltage V_p and output power P_p and the load resistance R_l, at different values of λ_m and fr. The results are shown in Figure 16 and Figure 17. A familiar conclusion can be made that with the increase of R_l, amplitude of output voltage V_p increases to an ultimate limit while amplitude of output power P_p reaches its peak at some value of R_l.

A further plot is generated using the amplitudes of output voltage V_p and output power P_p versus line density ratio λ_m at different values of load resistance R_l and base excitation frequency fr, as shown in Figure 18 and Figure 19. It
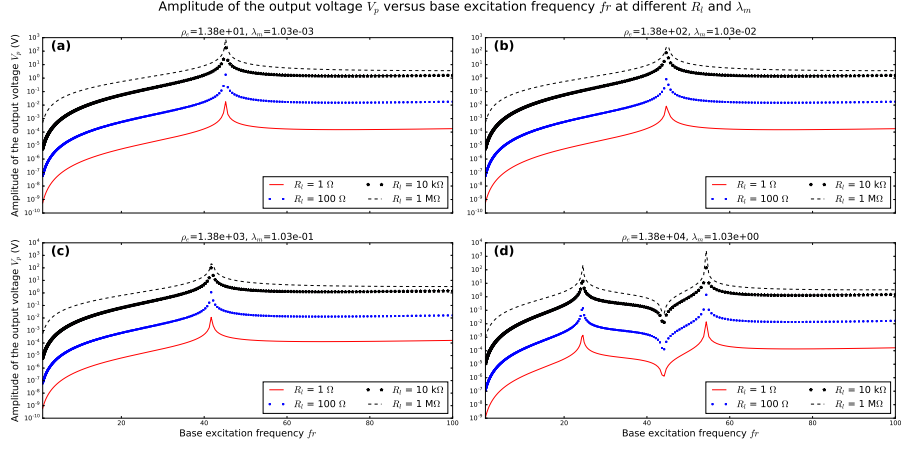
18

Figure 14: Output voltage V_p (amplitude) of the piezoelectric energy harvester with flexible extension versus base excitation frequency fr at different line density ratio λ_m and load resistance R_l.
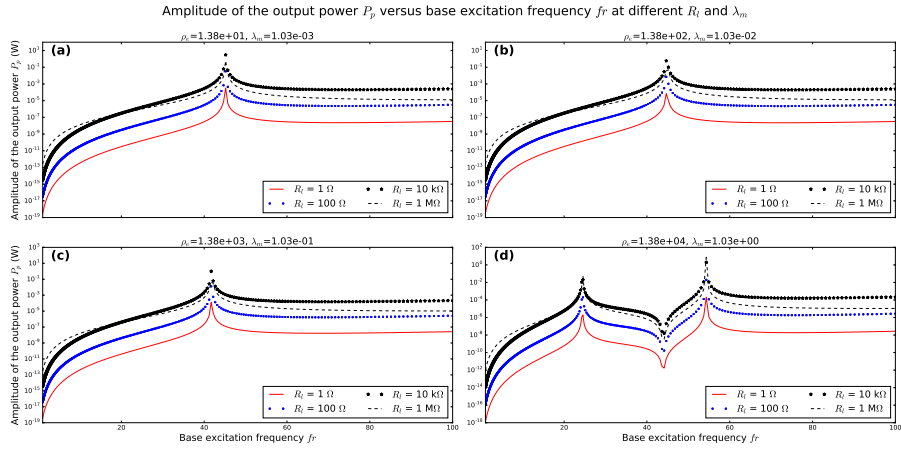

Figure 15: Output power P_p (amplitude) of the piezoelectric energy harvester with flexible extension versus base excitation frequency fr at different line density ratio λ_m and load resistance R_l.
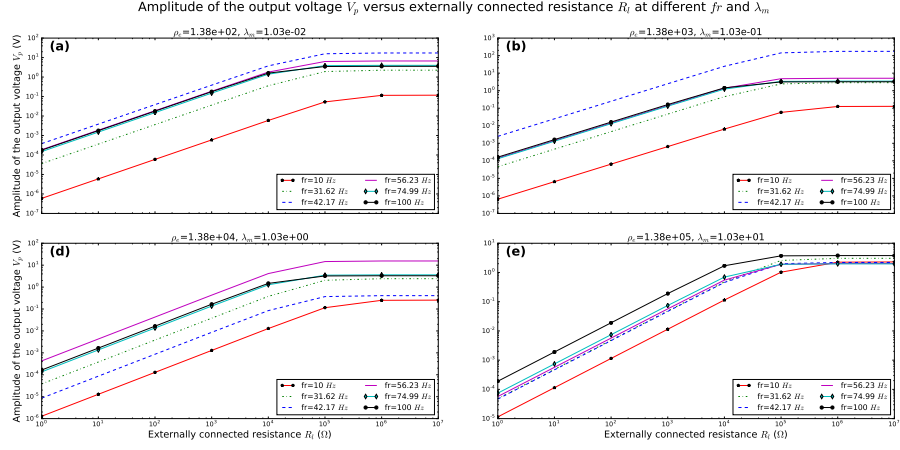
Figure 16: Output voltage V_p (amplitude) of the piezoelectric energy harvester with flexible extension versus load resistance R_l at different frequency fr and line density ratio λ_m.
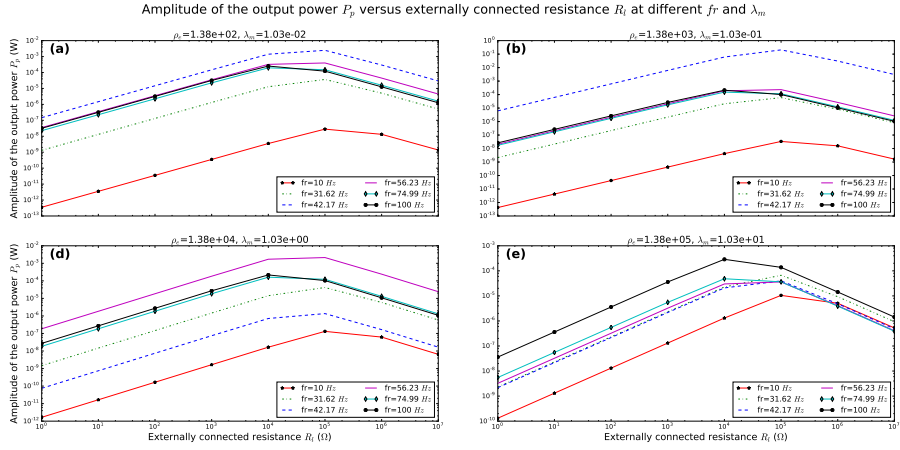

Figure 17: Output power P_p (amplitude) of the piezoelectric energy harvester with flexible extension versus load resistance R_l at different frequency fr and line density ratio λ_m.

is obvious that for low base excitation frequency, like $fr = 1\ Hz$, V_p and P_p increase with respect to λ_m. For the case of $fr = 31.62\ Hz$, V_p and P_p changes little with respect to λ_m, compared with the cases of smaller λ_m. For the case of $fr = 41.27\ Hz$, a significant change of V_p and P_p can be seen with respect to λ_m. While for the case of $fr = 100\ Hz$, the change becomes negligible again. That is to say, at the frequency around the resonant frequency in the considered range, the change of line density ratio λ_m is helpful to improve the performance of the proposed piezoelectric energy harvester with flexible extension. In the other cases, the change of λ_m won't help too much.
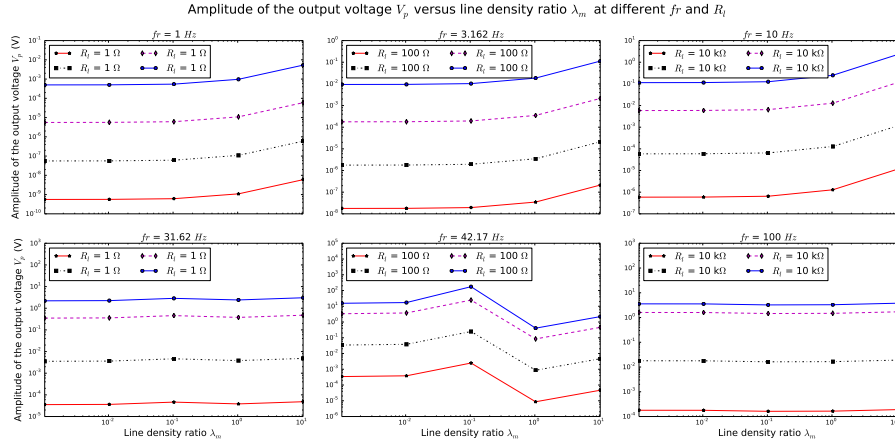

Figure 18: Output voltage V_p (amplitude) of the piezoelectric energy harvester with flexible extension versus line density ratio λ_m at different frequency fr and load resistance R_l. legend to be revised

5. Conclusion and Discussion

Here in this contribution, we investigate the method of using elastic extension to tune the energy harvesting performance of classic piezoelectric cantilever energy harvesters. Dynamic model of the proposed method is established and transformed into a boundary value problem. Simulations are done to figure out the influence several system parameters, like length ratio λ_l, bending stiffness ratio λ_B, and line density ratio λ_m, upon the performance of the piezoelectric energy harvester with elastic extensions.

Firstly, it is found that by changing the parameter values, we can introduce extra resonant modes in the considered frequency range. And these resonant modes are potential for energy harvesting applications as the output level is usable. As engineering energy harvesting applications rely on resonant modes wot work, this means that we can expand the work range of energy harvesters by adding elastic extensions.
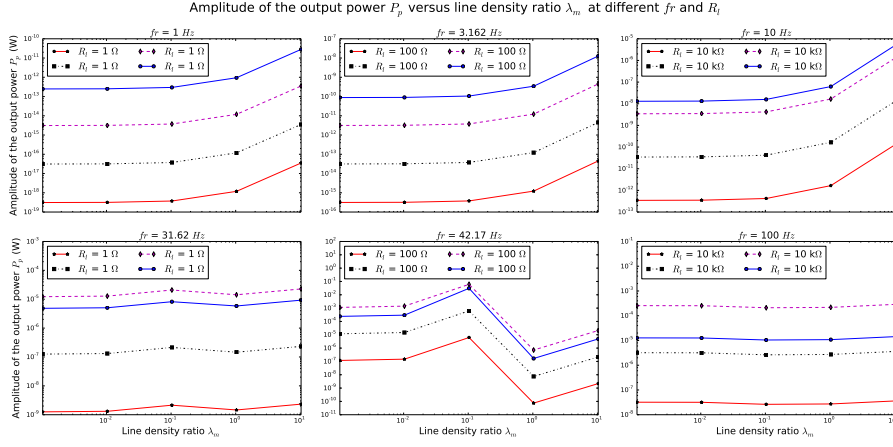
21

Figure 19: Output power P_p (amplitude) of the piezoelectric energy harvester with flexible extension versus line density ratio λ_m at different frequency fr and load resistance R_l. legend to be revised

Secondly, energy harvesting performance of a classical piezoelectric energy harvester can be tuned by elastic extension. It is seen from the simulation results that by changing parameter values, the introduced resonant mode can have a strong interaction with the originally resonant mode of a piezoelectric energy harvester. In this way, we see this system as a coupled oscillating system. By changing parameter values, the energy input into the whole system can be concentrated in one single oscillator. In that way, the output performance of the piezoelectric energy harvester is somehow strengthened and improved.

Thirdly, the tuning effect of the elastic extension is the result of the combine action of three parameters λ_l, λ_B, and λ_m. The increase of λ_l and λ_m tends to increase the number of introduced resonant modes, while the increase of λ_B tends to decrease it. Thus to better improve the performance of a piezoelectric energy harvester, a comprehensive study is yet to be done to figure out the best parameter set. In this sense, the asymptotic of the problem is necessary and will be the topic of future research.

Reference

[1] Zhou M, Al-Furjan MSH, Zou J, Liu W. A review on heat and mechanical energy harvesting from human–Principles, prototypes and perspectives. Renewable and Sustainable Energy Reviews. 2018;82:3582–3609.

[2] Dagdeviren C, Li Z, Wang ZL. Energy harvesting from the animal/human body for self-powered electronics. Annual Review of Biomedical Engineering. 2017;19:85–108.

[3] Safaei M, Sodano HA, Anton SR. A review of energy harvesting using piezoelectric materials: State-of-the-art a decade later (2008-2018). Smart Materials and Structures. 2019;.

[4] Liu H, Zhong J, Lee C, Lee SW, Lin L. A comprehensive review on piezoelectric energy harvesting technology: Materials, mechanisms, and applications. Applied Physics Reviews. 2018;5(4):041306.

[5] Cepnik C, Lausecker R, Wallrabe U. Review on electrodynamic energy harvestersa classification approach. Micromachines. 2013;4(2):168–196.

[6] Tan Y, Dong Y, Wang X. Review of MEMS electromagnetic vibration energy harvester. Journal of Microelectromechanical Systems. 2016;26(1):1–16.

[7] Khan FU, Qadir MU. State-of-the-art in vibration-based electrostatic energy harvesting. Journal of Micromechanics and Microengineering. 2016;26(10):103001.

[8] Suzuki Y. Recent progress in MEMS electret generator for energy harvesting. IEEJ Transactions on Electrical and Electronic Engineering. 2011;6(2):101–111.

[9] Sodano HA, Inman DJ, Park G. A review of power harvesting from vibration using piezoelectric materials. Shock and Vibration Digest. 2004;36(3):197–206.

[10] Fan FR, Tang W, Wang ZL. Flexible nanogenerators for energy harvesting and self-powered electronics. Advanced Materials. 2016;28(22):4283–4305.

[11] Wang ZL, Chen J, Lin L. Progress in triboelectric nanogenerators as a new energy technology and self-powered sensors. Energy & Environmental Science. 2015;8(8):2250–2282.

[12] Anton SR, Sodano HA. A review of power harvesting using piezoelectric materials (2003–2006). Smart materials and Structures. 2007;16(3):R1.

[13] Erturk A, Inman DJ. A distributed parameter electromechanical model for cantilevered piezoelectric energy harvesters. Journal of vibration and acoustics. 2008;130(4):041002.

[14] Erturk A, Inman DJ. An experimentally validated bimorph cantilever model for piezoelectric energy harvesting from base excitations. Smart materials and structures. 2009;18(2):025009.

[15] Goldschmidtboeing F, Woias P. Characterization of different beam shapes for piezoelectric energy harvesting. Journal of micromechanics and microengineering. 2008;18(10):104013.

[16] Fu H, Chen G, Bai N. Electrode coverage optimization for piezoelectric energy harvesting from tip excitation. Sensors. 2018;18(3):804.

[17] Kim M, Dugundji J, Wardle BL. Effect of electrode configurations on piezoelectric vibration energy harvesting performance. Smart Materials and Structures. 2015;24(4):045026.

[18] Liao Y, Sodano HA. Optimal placement of piezoelectric material on a cantilever beam for maximum piezoelectric damping and power harvesting efficiency. Smart materials and structures. 2012;21(10):105014.

[19] Patel R, McWilliam S, Popov AA. A geometric parameter study of piezoelectric coverage on a rectangular cantilever energy harvester. Smart Materials and Structures. 2011;20(8):085004.

[20] Yildirim T, Ghayesh MH, Li W, Alici G. A review on performance enhancement techniques for ambient vibration energy harvesters. Renewable and Sustainable Energy Reviews. 2017;71:435–449.

[21] Tran N, Ghayesh MH, Arjomandi M. Ambient vibration energy harvesters: A review on nonlinear techniques for performance enhancement. International Journal of Engineering Science. 2018;127:162–185.

[22] Zhou CQXZ Maoying, Wang W. Piezoelectric wind energy harvesting device based on the inverted cantilever beam with leaf-inspired extensions. AIP Advances. 2019;9:035213.

[23] Park CH. Dynamics modelling of beams with shunted piezoelectric elements. Journal of Sound and vibration. 2003;268(1):115–129.

[24] Timoshenko S. Vibration problems in engineering. Wiley; 1974.

[25] Maurini C, Porfiri M, Pouget J. Numerical methods for modal analysis of stepped piezoelectric beams. Journal of Sound and Vibration. 2006;298(4-5):918–933.

[26] Wu JJ. A generalized harmonic balance method for forced non-linear oscillations: the subharmonic cases. Journal of Sound and Vibration. 1992;159(3):503–525.

[27] Driscoll TA, Hale N, Trefethen LN. Chebfun guide. Pafnuty Publications, Oxford; 2014.

[28] Warlimont H, Martienssen W. Springer Handbook of Materials Data. Springer; 2018.

[29] Dean JA. Lange's handbook of chemistry. New york; London: McGraw-Hill, Inc.; 1999.